Progress In Electromagnetics Research M, Vol. 72, 49–59, 2018

Isolation Enhancement Using a Novel Array-Antenna Decoupling Surface for Microstrip Antennas

Zicheng Niu*, Hou Zhang, Qiang Chen, and Tao Zhong

Abstract—A novel array-antenna decoupling surface (ADS) for mutual coupling reduction in microstrip patch antenna is proposed in this paper. The proposed ADS is composed of a group of primary reflector patches and a pair of rectangular and T-shaped secondary reflector patches. Through generating the reflected waves with equal magnitude but out of phase of the coupling waves, the isolation of the antenna elements could be significantly improved by the novel proposed ADS. Then, for verification, a two-element microstrip antenna array covered by the proposed ADS with an edge-to-edge separation of $0.11\lambda_0$ (λ_0 is the wavelength of the operating frequency in free space) was designed and fabricated. As expected, the experimental results have demonstrated that an additional 40.4 dB isolation enhancement at the resonant frequency was achieved by the proposed ADS. Moreover, a much wider bandwidth of the isolation was also obtained than that of return loss of 10 dB. In addition, a gain improvement of 0.95 dB was achieved at 2.45 GHz by utilizing the novel ADS. Thus, the decoupling structure can be applied to multiple-input multiple-output (MIMO) systems for its simple structure and high isolation providing.

1. INTRODUCTION

MIMO has been widely used in many wireless communication systems, such as WLAN, WIMAX and LTE, due to its advantages, such as improved channel capacity and reliability. Meanwhile, WLAN has become one of the main ways to carry network traffic due to its advantages of low cost, fast data transmission and easy deployment. MIMO system requires multiple antennas to suit for high channel capacity and high data rate [1, 2]. However, with the increase of the number of antennas, the mutual coupling between antenna elements has become an issue that cannot be neglected. Mutual coupling leads to the deterioration of antenna performance, including mismatching impedance and degrading radiation efficiency [3]. Because the mutual coupling between antenna elements can cause interference to the signal, low mutual coupling demand between the antenna elements becomes especially important.

The cause of mutual coupling includes spatial field coupling, common current coupling, feeding coupling and the like. In recently published literatures, several approaches have proposed to reduce the mutual coupling between two antenna elements. In [4] and [5], electromagnetic band-gap (EBG) structures which have band-stop feature are proposed to suppress the surface wave propagation for alleviating the mutual coupling effect. However, due to deploying the periodic structures between the antenna elements, the distance between the antenna elements has to be expanded. In [6–8], the isolation enhancement through suppressing the common ground current is achieved by applying a defected grounded structure (DGS). Nevertheless, it reduces antenna front-to-back ratio and lower antenna gain. In [9], the meta-surface consists of periodic square split ring resonators. It is suspended above the antenna array, and a satisfactory isolation enhancement is attained. However, due to the change of medium parameters, the matching of the microstrip antenna becomes worse. In [10, 11], the

Received 5 July 2018, Accepted 6 August 2018, Scheduled 17 August 2018
* Corresponding author: Zicheng Niu (nzc585@126.com).
The authors are with the Air and Missile Defense College, Air Force Engineering University, Xi'an 710051, China.

array-antenna decoupling surface (ADS) is proposed and applied to the antenna arrays with isolation enhancement. The ADS has the advantage that maintains the matching conditions of the original antenna, increasing the radiation gain and process conveniently.

In this paper, a novel ADS is proposed to reduce the mutual coupling between two patch antennas. It consists of primary reflector patches and a pair of rectangular and T-shaped secondary reflector patches. The isolation enhancement is realized by producing reflected waves with equal magnitude but out of phase of the coupling waves. For verification, a two-element microstrip antenna array covered by the proposed ADS with an edge-to-edge separation of $0.11\lambda_0$ was designed and fabricated. The proposed ADS achieves a high isolation enhancement within working bandwidth, though the advantages of the low profile of the patch antenna get damaged. The radiation gain improvement is also made in this design.

The paper is organized as follows. Section 2 presents the design and characterization of the ADS. Section 3 presents the numerical optimization of structure parameters. Section 4 presents the simulated and measured results. Section 5 presents conclusion of the paper.

2. NOVEL ADS DESIGN

The ADS consists of a plurality of metal reflection strips. These metal strips are divided into a primary reflector which provides the main reflected waves and a secondary reflector which compensates the missing components of the main reflected waves. As shown in Fig. 1, the ADS with a primary reflector and a secondary reflector is suspended above the two-element antenna array. The ADS improves the isolation between the antenna elements through generating the reflected waves which have equal magnitude but out of phase coupling waves. A well-designed ADS ought to satisfy the following conditions

$$|S_{21}^{\text{reflect}}| = |S_{21}^{\text{array}}| \tag{1}$$

$$\text{Phase}(S_{21}^{\text{reflect}}) - \text{Phase}(S_{21}^{\text{array}}) = \pm n\pi \ (n = 1, 3, 5, \ldots) \tag{2}$$

where S_{21}^{array} is the transmission coefficient of the microstrip antenna array without ADS, and S_{21}^{reflect} is the transmission coefficient of the reflected waves generated by the ADS, which is transmitted from antenna 1 to antenna 2.

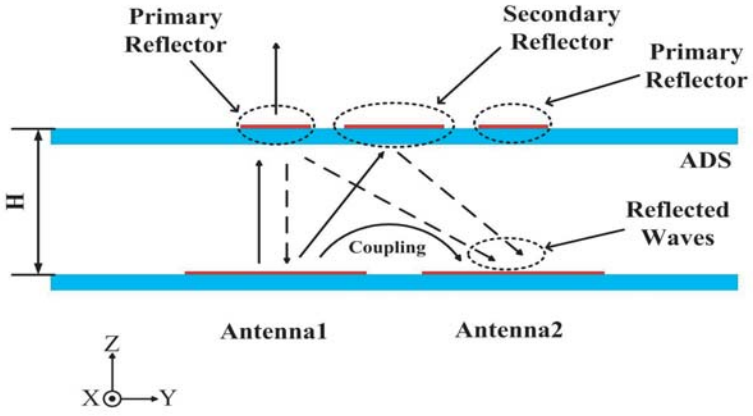

Figure 1. Field distribution of two coupled antenna array with the ADS.

In order to show the design process of the proposed ADS, three ADS prototypes are depicted in Fig. 2. Among them, (a) which only consists of the primary reflectors is proposed by Wu et al. in [10]. From this paper, we know that the primary reflector patches create the main reflected waves, and the secondary reflector patches compensate the missing components of the main reflected waves. So, the ADS which contains a pair of rectangular and T-shaped secondary reflectors is designed. Adding the

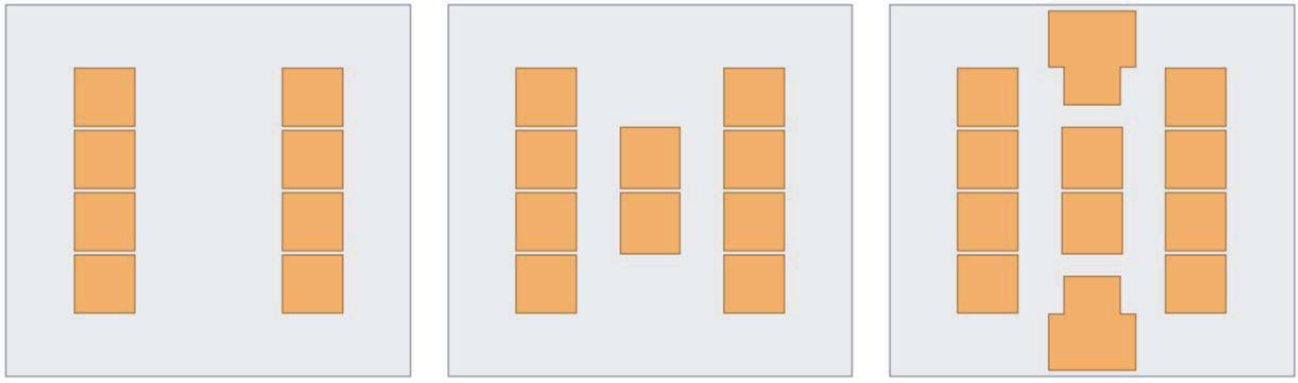

Figure 2. Evolution of the proposed ADS design. (a) Stage 1: The ADS only consists of the primary reflector patches. (b) Stage 2: The ADS with a pair of rectangular secondary reflector patches. (c) Stage 3: The ADS consists of a group of primary reflector patches, a pair of rectangular and T-shaped secondary reflector patches.

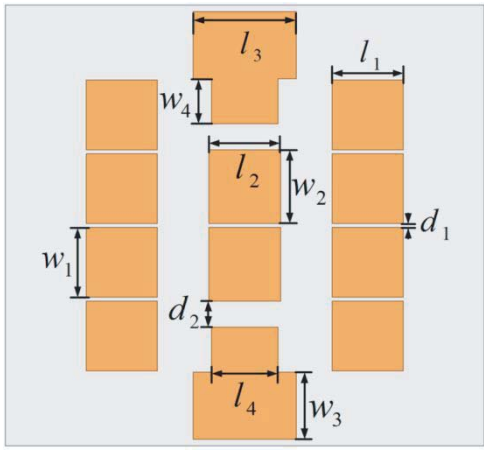

Figure 3. Schematic diagram of the proposed ADS.

proposed secondary reflector patches not only does not change the area of the ADS before, but also obtains better isolation.

The proposed ADS structure is shown in Fig. 3. The substrate used for the ADS is with thickness of 1 mm, dielectric constant of 2.65, and loss tangent of 0.001. The design, characterization, and optimization of the proposed ADS are done by HFSS 13.0. The optimized dimensions of the proposed ADS are $w_1 = 15.5$ mm, $l_1 = 16$ mm, $w_2 = 16.4$ mm, $l_2 = 16$ mm, $w_3 = 15$ mm, $l_3 = 23$ mm, $w_4 = 10$ mm, $l_4 = 15$ mm, $d_1 = 1$ mm, $d_2 = 6.1$ mm.

In order to better demonstrate the effect of the proposed ADS for mutual coupling suppression, a two-element microstrip antenna array is covered by the proposed ADS as shown in Fig. 4. The dimensions of the microstrip antenna array are $w_p = 42$ mm, $l_p = 37$ mm, $R_1 = 1.2$ mm, $R_2 = 3$ mm, $l_c = 5.2$ mm, $d = 13$ mm and $t = 1$ mm. The antenna array is also placed upon a 1 mm thick substrate with dielectric constant 2.65 and loss tangent 0.001. Both the antennas are excited by a coaxial connector with 50 Ω impedance. The microstrip antennas operate at 2.45 GHz and have an edge-to-edge separation of $0.11\lambda_0$. The proposed ADS is suspended above the antenna array at a height of 38 mm ($0.31\lambda_0$), and each group of primary reflector patches is placed right above its corresponding microstrip antenna element as shown in Fig. 4(b).

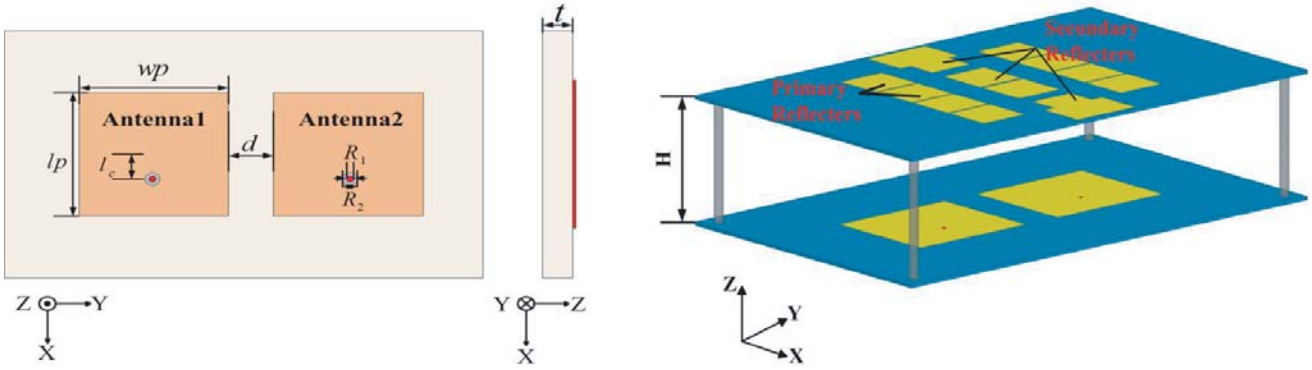

(a) (b)

Figure 4. (a) Schematic diagram of the two-element microstrip antenna array; (b) Implementation of the proposed ADS on the microstrip antenna array.

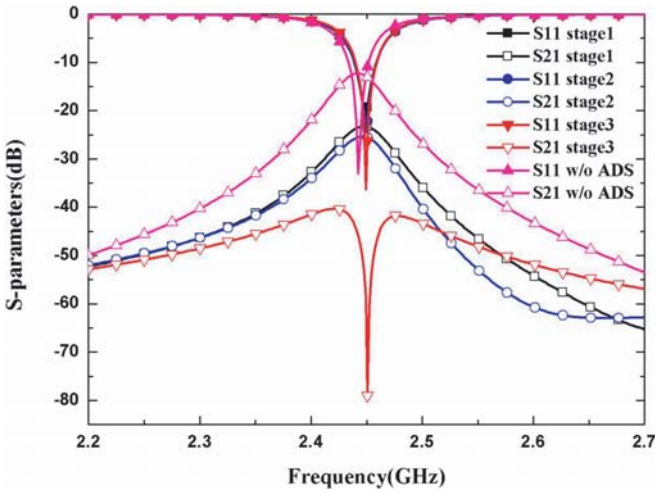

Figure 5. Simulated S-parameters for stage 1–3 and without ADS array.

Figure 5 shows the reflection and transmission characteristics of the 1×2 microstrip antenna array with the ADS during various stages of evolution. As shown in Fig. 5, the isolation of stage 1 is 23 dB at 2.45 GHz. When adding a pair of rectangular secondary reflectors, the isolation is only increased 3 dB (from 23 dB to 26 dB). However, by adding a pair of T-shaped secondary reflectors, the isolation between the antenna elements reaches 78 dB at 2.45 GHz, which is increased 55 dB compared to stage 1. It can also be seen that with the continuous improvement of the ADS structure, the matching of antenna 1 at the central frequency is getting better and better, but the bandwidth of return loss of 10 dB has hardly changed.

Figure 6 depicts the distribution of the electric filed contours on a cutting surface in XOZ plane under different phase conditions. It can be seen from Figs. 6(a), (b), (c) and (d) that no matter which ADS is loaded on the antenna array, the mutual coupling between the two antennas decreases compared to the array without ADS because the reflectors can provide reflected waves with equal magnitude but out of phase coupling waves. With the continuous improvement of ADS, the power of antenna 1 coupled to antenna 2 is reduced. Due to the addition of the rectangular secondary reflectors, there is a coupling effect of energy between the main reflectors and rectangular secondary reflectors, but the energy coupling is small, so the isolation between the antenna elements is only slightly improved as shown in Fig. 6(c). By comparison of Figs. 6(c) and (d), it is shown that the mutual coupling decreases significantly after adding T-shaped secondary reflectors. The reason for the significant increase in isolation is that after

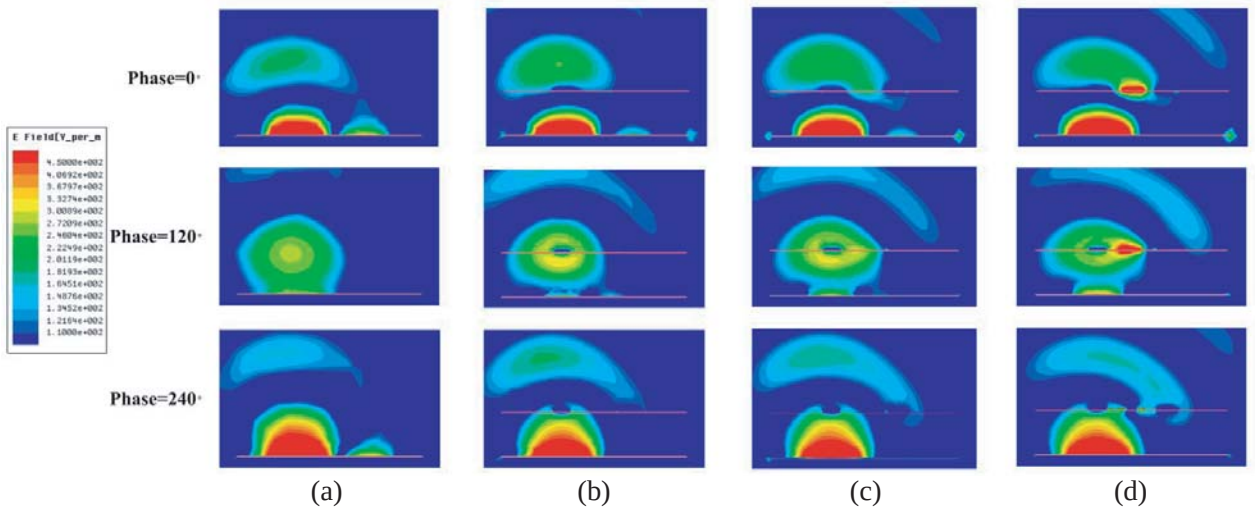

Figure 6. Simulated electric filed contours on a cutting surface in XOZ plane for array at 2.45 GHz (Antenna 1 is excited while Antenna 2 with matched load; (a) without ADS; (b) stage 1; (c) stage 2 and (d) stage 3.

loading T-shaped secondary reflectors, there is a coupling effect of energy between the rectangular secondary reflectors and primary reflectors. Although the direction of the beam is slightly affected, the isolation between antenna elements is greatly improved.

3. PARAMETERS ANALYSIS

In Section 2, the effects of the interaction of reflectors on the isolation are discussed. To further study the influence of the secondary reflectors on the coupling waves among the antenna elements, the parameters of the secondary reflectors are analyzed in this section.

3.1. Parameters Analysis of the Rectangular Secondary Reflectors

Figure 7 shows two clusters S_{21} curves with respect to different widths of the rectangular secondary reflectors, w_2, and lengths of the rectangular secondary reflectors, l_2. With the increase of w_2, which

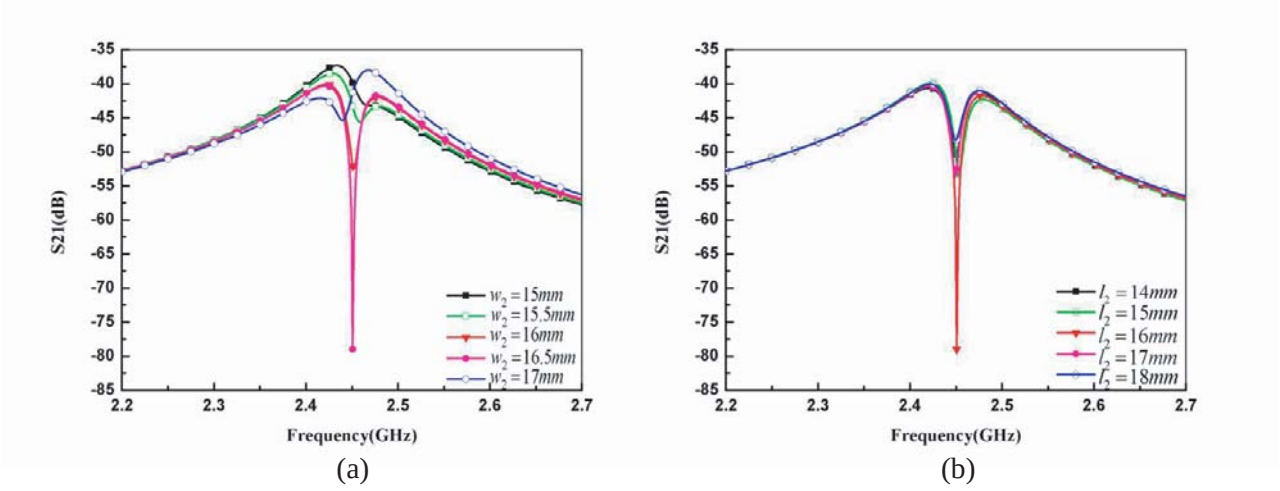

Figure 7. (a) Simulated S_{21} of the antenna array with ADS with respect to different w_2 — the width of the rectangular secondary reflector; (b) Simulated S_{21} of the antenna array with ADS with respect to different l_2 — the length of the rectangular secondary reflector.

is the width of the rectangular secondary reflector, the distance between it and the T-shaped reflector is gradually reduced, and part of the power is gathered between the two plates to produce resonance, which causes the maximum isolation to move to the lower frequency as given in Fig. 7(a). However, as the length of the rectangular secondary reflector changes, the maximum isolation is not offset at the center frequency in Fig. 7(b). It can be seen that the length of the rectangular secondary reflector only changes the maximum isolation at the central frequency.

3.2. Parameters Analysis of the T-Shaped Secondary Reflectors

As depicted in Figs. 8(b) and (d), it can be perceived that l_3 — the length of the T-shaped secondary reflector and l_4 — the length of protruding part of the T-shaped secondary reflector only change the maximum isolation at the central frequency but does not change the frequency at which the maximum isolation is located. As can be seen from Fig. 8(a) and Fig. 8(c), with the increase of w_3 — the width of T-shaped reflectors and w_4 — the width of the protruding part of the T-shaped secondary reflector, the maximum isolation moves to the lower frequency. This is because not only the power is concentrated

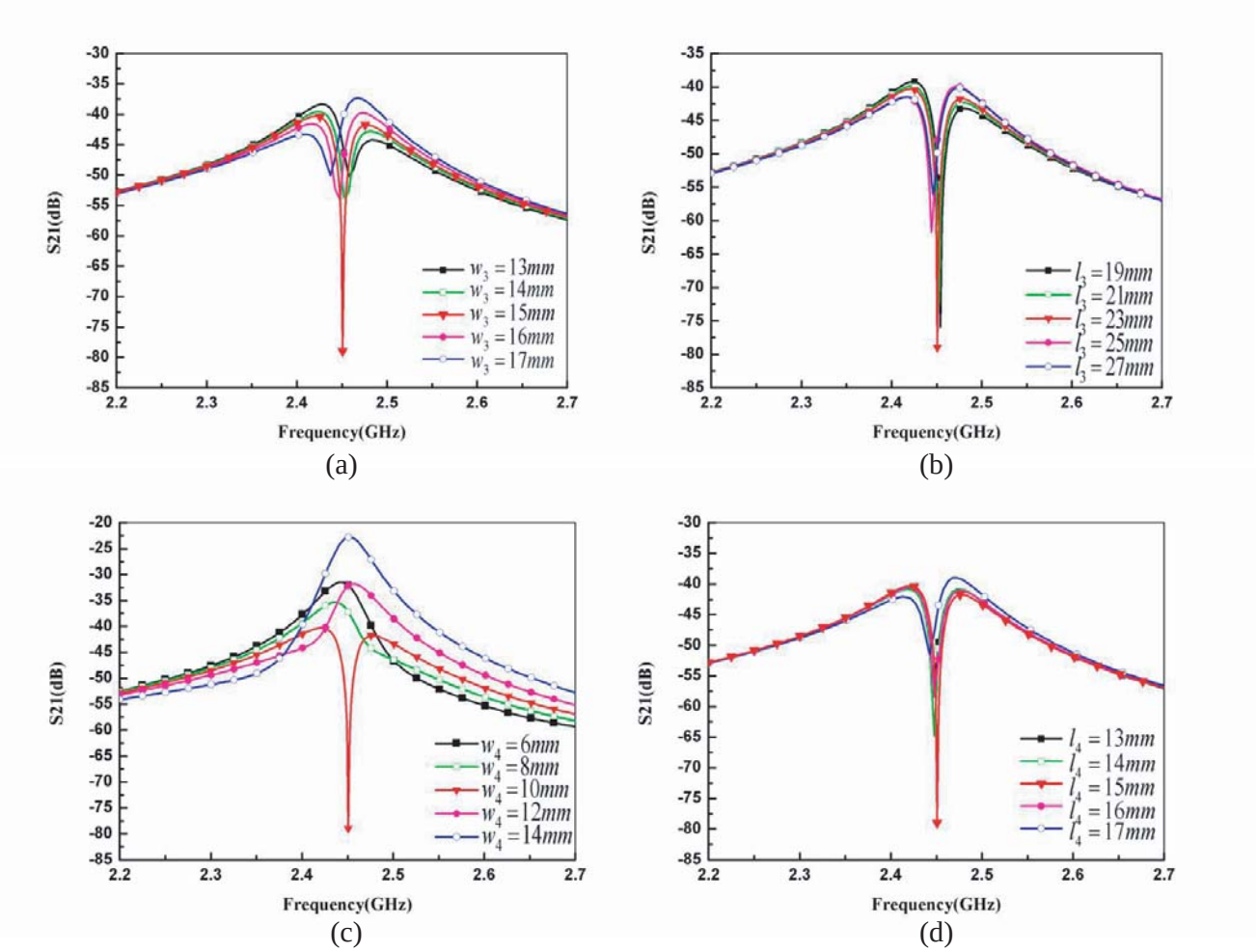

Figure 8. (a) Simulated S_{21} of the antenna array with ADS with respect to different w_3 — the width of the T-shaped secondary reflector; (b) Simulated S_{21} of the antenna array with ADS with respect to different l_3 — the length of the T-shaped secondary reflector; (c) Simulated S_{21} of the antenna array with ADS with respect to different w_4 — the width of the protruding part of the T-shaped secondary reflector; (d) Simulated S_{21} of the antenna array with ADS with respect to different l_4 — the length of the protruding part of the T-shaped secondary reflector.

between the T-shaped reflectors and rectangular secondary reflectors, but also there is power coupling between the T-shaped reflectors and rectangular primary reflectors.

4. SIMULATED AND MEASURED RESULTS

The simulated reflection and transmission coefficients of the microstrip antenna array with and without ADS are shown in Fig. 9. Since the antennas are compact, the array without ADS suffers from strong coupling, and the isolation between the antenna elements is only 13 dB at 2.45 GHz. After loading ADS, the mutual coupling at 2.45 GHz is found to be −78 dB. From the presented results, it is observed that the ADS provides additional 65 dB enhancement in the isolation between the antenna elements at 2.45 GHz. It also appears that the decoupling bandwidth reduced from −13 dB to −40 dB is much wider than return loss of 10 dB.

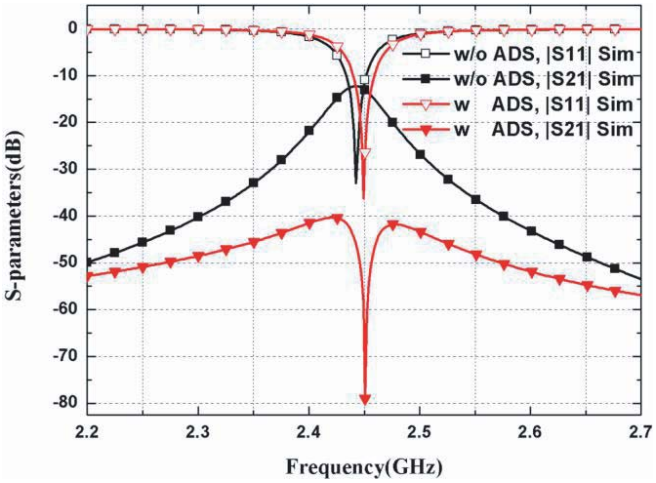

Figure 9. Simulated S-parameter characteristics of the microstrip antenna array with and without ADS.

To further verify properties of the proposed ADS, prototypes of the proposed ADS and referred microtrip antenna arrays are fabricated as shown in Fig. 10. As can be seen in Fig. 11, after adding the ADS, the center frequency of the array is shifted very little, which hardly affects the antenna matching. The measurement results in Fig. 11 demonstrate that the isolation of the array without ADS is 15.4 dB at 2.45 GHz, and the isolation using ADS reaches 55.8 dB (40.4 dB improved). In addition, the isolation

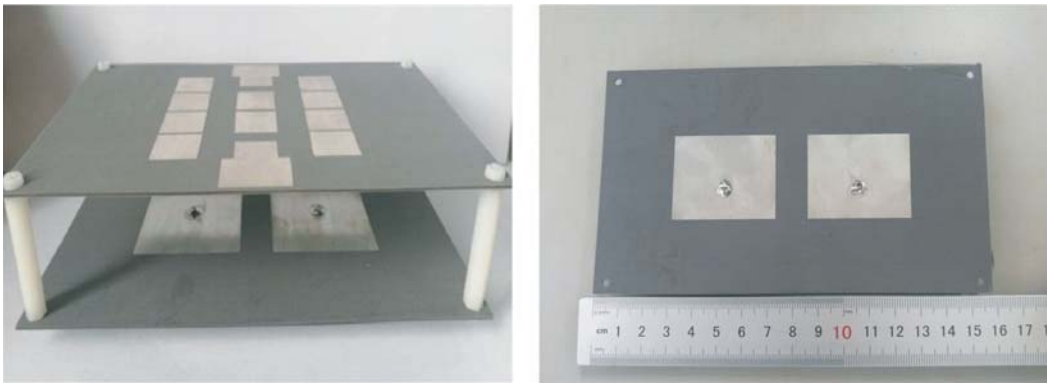

(a) (b)

Figure 10. Fabricated microstrip antenna array with and without ADS; (a) with ADS and (b) without ADS.

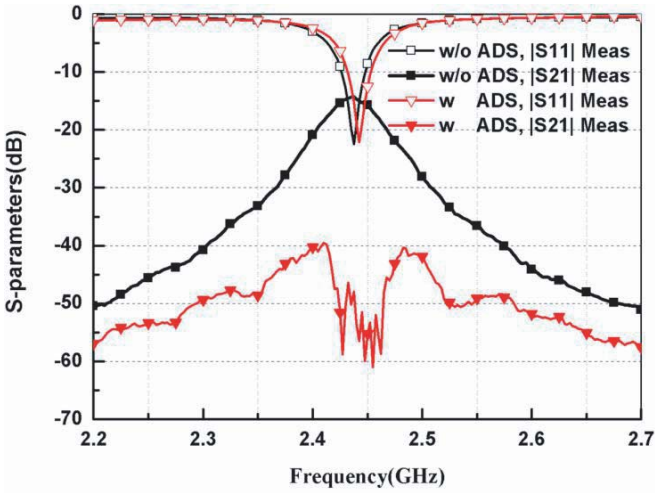

Figure 11. Measured S-parameter characteristics of the microstrip antenna array with and without ADS.

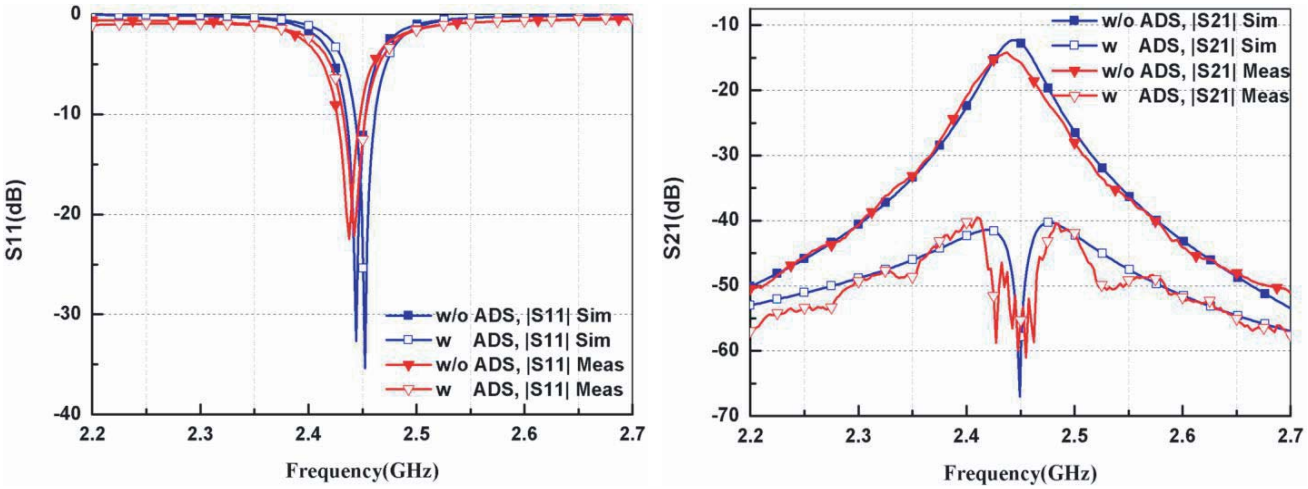

(a) (b)

Figure 12. Measured and simulated reflection and transmission coefficient for the arrays; (a) Reflection coefficient and (b) Transmission coefficient.

between the antenna elements can reach the maximum of 60 dB (44.7 dB improved) within the working bandwidth. Obviously, seen from Fig. 11, the bandwidth with isolation greater than 40 dB is much wider than return loss of 10 dB. The comparison between the measured and simulated reflection coefficients is shown in Fig. 12(a). It can be concluded that the measured results of the reflection coefficient of the antenna are basically consistent with the simulated results. As shown in Fig. 12(b), the measured transmission coefficient bandwidth, which is less than -40 dB, is increased. The measured and simulated radiation patterns of the arrays are shown in Figs. 13(a) and (b). As can be seen from Fig. 13(a), both the simulated and measured results show that the antenna reaches the maximum gain on the E plane at $\theta = 0$ deg. However, the backlobe level measurement of the antenna without ADS is smaller than the simulated result. Both the measured and simulated results show that the antenna reaches the maximum gain on the H plane at $\theta = 25$ deg, shown in Fig. 13(b). It can be concluded that the measured and simulated results agree well with each other. Figs. 14(a) and (b) show the measured gain of the antenna at $\varphi = 0$ deg and $\varphi = 90$ deg, respectively. As can be seen in Fig. 14(a), the antenna without ADS at $\theta = 0$ deg reaches the peak gain, which is 5.8 dB. It can been seen from Fig. 14(b) that after loading

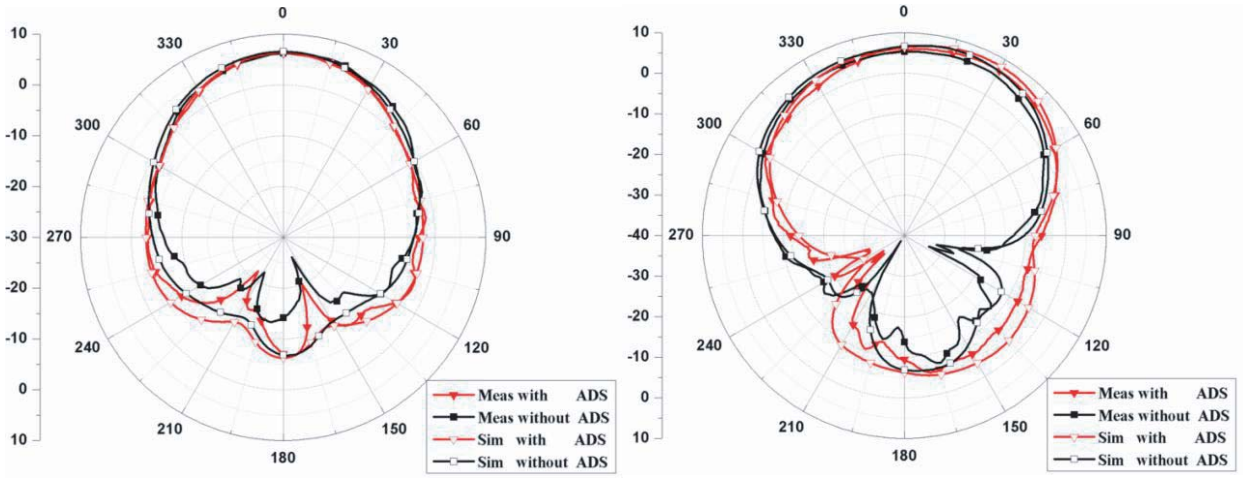

Figure 13. Measured and simulated radiation pattern for the arrays at 2.45 GHz with and without ADS (antenna 1 excited and antenna 2 terminated by 50 Ω); (a) E-plane and (b) H-plane.

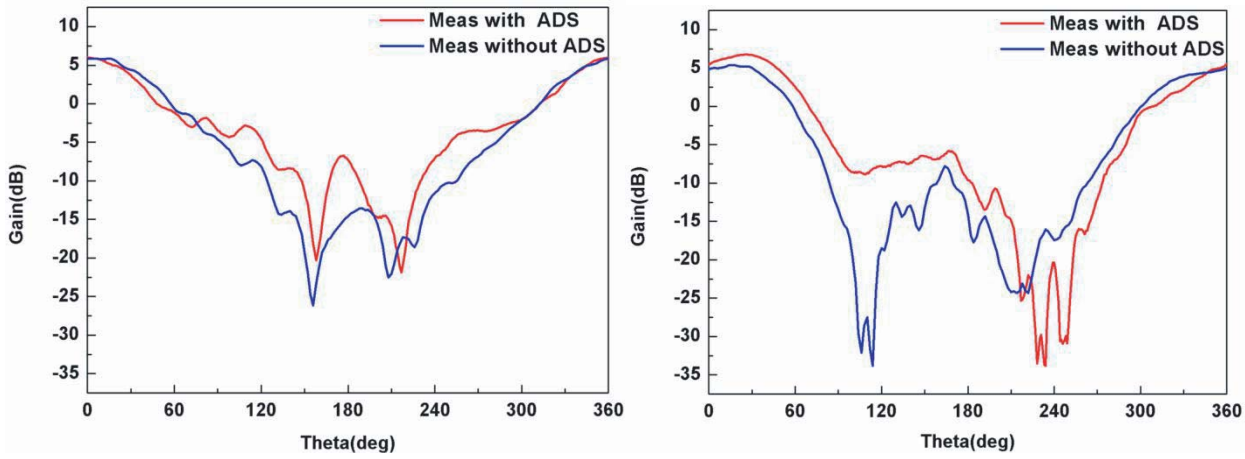

Figure 14. Measured gain for the arrays at 2.45 GHz with and without ADS (antenna 1 excited and antenna 2 terminated by 50 Ω); (a) $\varphi = 0$ deg and (b) $\varphi = 90$ deg.

Table 1. Performance comparison of the proposed ADS and high-isolation decoupling techniques used in recent published literatures.

Papers	Decoupling technique	f_0 (GHz)	Edge to Edge spacing (λ_0)	Maximum isolation improvement (dB)	Size (λ_0)
[12]	PCI	5.8	0.17	19.6	NA
[13]	Resonator	5.25	0.5	44	0.7×1
[14]	UC-EBG	5.05	0.22	16	0.5×0.8
[15]	PCR	3.5	0.07	26.2	0.6×0.8
Proposed	ADS	2.45	0.11	44.7	0.8×1.3

ADS, the antenna at $\theta = 25$ deg reaches the peak gain, which is 6.75 dB. Thus, it can be found from the measurement that the peak gain of the antenna with adding the proposed ADS is 0.95 dB higher than that of the arrays without ADS, improving from 5.8 dB to 6.75 dB.

Table 1 shows the decoupling techniques and their performances in recent published literature compared to the proposed ADS utilized in this paper. From comparisons, it can be seen that each decoupling mechanism has its own characteristics. From Table 1, although the size of the proposed antenna with ADS is larger than others, it can achieve excellent maximum isolation improvement at close range between antenna elements.

5. CONCLUSION

The paper presents a novel ADS structure where isolation property is remarkably improved in 1×2 microstrip antenna arrays. Through adding the secondary reflectors to compensate missing components of the main reflected waves, the isolation property improvement between the antenna elements can be easily made. To verify the simulations, the prototype of antenna array with ADS is fabricated and measured. The measured results show that the proposed ADS provides a maximum isolation enhancement from 15.3 to 60 dB (44.7 dB improved) within working bandwidth. Additionally, the gain improvement is 0.95 dB at the resonant frequency. So the proposed ADS structure provides an attractively alternative solution to the design of high isolation antenna arrays for Massive MIMO arrays.

REFERENCES

1. Vaughan, R. and J. B. Andersen, "Channels, propagation and antennas for mobile communications," *The Institution of Electrical Engineers*, 2003.
2. Foschini, G. J., "Layered space 2-time architecture for wireless communications in fading environment when using multi-element antennas," *Bell Labs Technology*, Vol. 1, 41–59, 1996.
3. Allen, J. L. and B. L. Diamond, "Mutual coupling in array antennas," Tech. Rep. 424 (ESD-TR-66-443), Lincoln Laboratory, M.I.T., Lexington, MA, 1966.
4. Yang, F. and Y. Rahmat-Samii, "Microstrip antennas integrated with electromagnetic band-gap (EBG) structures: A low mutual coupling design for array applications," *IEEE Transactions on Antennas and Propagation*, Vol. 51, No. 10, 2936s–2946, 2003.
5. Radhi, A. H., N. A. Aziz, R. Nilavalan, and H. S. Al-Raweshidy, "Mutual coupling reduction between two PIFA using uni-planar fractal based EBG for MIMO application," *2016 Loughborough Antennas & Propagation Conference (LAPC)*, 1–5, 2016.
6. Habashi, A., J. Naurinia, and C. Ghbadi, "A rectangular defected ground structure for reduction of mutual coupling between closely spaced microstrip antennas," *Proc. 20th Iranian Conf. Eng.*, 1347–1350, 2012.
7. Biswas, S. and D. Guha, "Stop-band characterization of an isolated DGS for reducing mutual coupling between adjacent antenna elements and experimental verification for dielectric resonator antenna array," *International Journal of Electronics and Communications*, Vol. 67, No. 4, 319–322, 2013.
8. Hou, D. B., S. Xiao, B. Z. Wang, L. Jiang, J. Wang, and W. Hong, "Elimination of scan blindness with compact defected ground structures in microstrip phased array," *IET Microwaves Antennas and Propagation*, Vol. 3, No. 2, 269–275, 2009.
9. Wang, Z. Y., L. Y. Zhao, Y. M. Cai, S. F. Zheng, and Y. Z. Yin, "A meta-surface antenna array decoupling (MAAD) method for mutual coupling reduction in a MIMO antenna system," *Scientific Reports*, Vol. 8, No. 3152, 2018.
10. Wu, K. L., N. Chang, W. X. Mei, and Z. Y. Zhang, "Array-antenna decoupling surface," *IEEE Transactions on Antennas and Propagation*, Vol. 65, No. 12, 6728–6738, 2017.
11. Wei, C. N. and K. L. Wu, "Array-antenna decoupling surfaces for Quasi-Yagi antenna arrays," *Antennas and Propagation & USNC/URSI National Radio Science Meeting*, 2103–2104, 2017.
12. Cheng, Y. F., X. Ding, W. Shao, and B. Z. Wang, "Reduction of mutual coupling between patch antennas using a polarization-conversion isolator," *IEEE Antennas Wireless Propagation Letters*, Vol. 16, 1257–1260, 2017.

13. Ghosh, C.-K., "A compact 4-channel microstrip MIMO antenna with reduced mutual coupling," *International Journal of Electronics and Communications*, Vol. 70, 873–879, 2016.
14. Yang, X., Y. Liu, Y. X. Xu, and S. X. Gong, "Isolation enhancement in patch antenna array with fractal UC-EBG structure and cross slot," *IEEE Antennas Wireless Propagation Letters*, Vol. 16, 2175–2178, 2017.
15. Vishvaksenan, K. S., K. Mithra, R. Kalaiarasan, and K. S. Raj, "Mutual coupling reduction in microstrip patch antenna arrays using parallel coupled-line resonators," *IEEE Antennas Wireless Propagation Letters*, Vol. 16, 2146–2149, 2017.